F. A. Aharonian, ... G. P. Rowell, ... S. J. Wagner [et al].
Search for TeV emission from the region around PSR B1706-44 with the HESS experiment.
Astronomy and Astrophysics, 2005; 432 (1):L9-L12

http://hdl.handle.net/2440/37480

Search for TeV emission from the region around PSR B1706–44 with the HESS experiment

F. Aharonian[1], A. G. Akhperjanian[2], K.-M. Aye[3], A. R. Bazer-Bachi[4], M. Beilicke[5], W. Benbow[1], D. Berge[1],
P. Berghaus[6,*], K. Bernlöhr[1,7], C. Boisson[8], O. Bolz[1], C. Borgmeier[7], I. Braun[1], F. Breitling[7], A. M. Brown[3],
J. Bussons Gordo[9], P. M. Chadwick[3], L.-M. Chounet[10], R. Cornils[5], L. Costamante[1,20], B. Degrange[10],
A. Djannati-Ataï[6], L. O'C. Drury[11], G. Dubus[10], T. Ergin[7], P. Espigat[6], F. Feinstein[9], P. Fleury[10], G. Fontaine[10],
Y. Fuchs[12], S. Funk[1], Y. A. Gallant[9], B. Giebels[10], S. Gillessen[1], P. Goret[13], C. Hadjichristidis[3], M. Hauser[14],
G. Heinzelmann[5], G. Henri[12], G. Hermann[1], J. A. Hinton[1], W. Hofmann[1], M. Holleran[15], D. Horns[1],
O. C. de Jager[15], I. Jung[1,14,**], B. Khélifi[1], Nu. Komin[7], A. Konopelko[1,7], I. J. Latham[3], R. Le Gallou[3],
A. Lemière[6], M. Lemoine[10], N. Leroy[10], T. Lohse[7], A. Marcowith[4], C. Masterson[1,20], T. J. L. McComb[3],
M. de Naurois[16], S. J. Nolan[3], A. Noutsos[3], K. J. Orford[3], J. L. Osborne[3], M. Ouchrif[16,20], M. Panter[1], G. Pelletier[12],
S. Pita[6], G. Pühlhofer[1,14], M. Punch[6], B. C. Raubenheimer[15], M. Raue[5], J. Raux[16], S. M. Rayner[3],
I. Redondo[10,20,***], A. Reimer[17], O. Reimer[17], J. Ripken[5], L. Rob[18], L. Rolland[16], G. Rowell[1], V. Sahakian[2],
L. Saugé[12], S. Schlenker[7], R. Schlickeiser[17], C. Schuster[17], U. Schwanke[7], M. Siewert[17], H. Sol[8], R. Steenkamp[19],
C. Stegmann[7], J.-P. Tavernet[16], R. Terrier[6], C. G. Théoret[6], M. Tluczykont[10,20], G. Vasileiadis[9], C. Venter[15],
P. Vincent[16], B. Visser[15], H. J. Völk[1], and S. J. Wagner[14]

[1] Max-Planck-Institut für Kernphysik, PO Box 103980, 69029 Heidelberg, Germany
    e-mail: Bruno.Khelifi@mpi-hd.mpg.de
[2] Yerevan Physics Institute, 2 Alikhanian Brothers St., 375036 Yerevan, Armenia
[3] University of Durham, Department of Physics, South Road, Durham DH1 3LE, UK
[4] Centre d'Étude Spatiale des Rayonnements, CNRS/UPS, 9 Av. du Colonel Roche, BP 4346, 31029 Toulouse Cedex 4, France
[5] Universität Hamburg, Institut für Experimentalphysik, Luruper Chaussee 149, 22761 Hamburg, Germany
[6] Physique Corpusculaire et Cosmologie, IN2P3/CNRS, Collège de France, 11 place Marcelin Berthelot,
    75231 Paris Cedex 05, France
[7] Institut für Physik, Humboldt-Universität zu Berlin, Newtonstr. 15, 12489 Berlin, Germany
[8] LUTH, UMR 8102 du CNRS, Observatoire de Paris, Section de Meudon, 92195 Meudon Cedex, France
[9] Groupe d'Astroparticules de Montpellier, IN2P3/CNRS, Université Montpellier II, CC85, Place Eugène Bataillon,
    34095 Montpellier Cedex 5, France
[10] Laboratoire Leprince-Ringuet, IN2P3/CNRS, Ecole Polytechnique, 91128 Palaiseau, France
[11] Dublin Institute for Advanced Studies, 5 Merrion Square, Dublin 2, Ireland
[12] Laboratoire d'Astrophysique de Grenoble, INSU/CNRS, Université Joseph Fourier, BP 53, 38041 Grenoble Cedex 9, France
[13] Service d'Astrophysique, DAPNIA/DSM/CEA, CE Saclay, 91191 Gif-sur-Yvette, France
[14] Landessternwarte, Königstuhl, 69117 Heidelberg, Germany
[15] Unit for Space Physics, North-West University, Potchefstroom 2520, South Africa
[16] Laboratoire de Physique Nucléaire et de Hautes Energies, IN2P3/CNRS, Universités Paris VI & VII, 4 place Jussieu,
    75231 Paris Cedex 05, France
[17] Institut für Theoretische Physik, Lehrstuhl IV: Weltraum und Astrophysik, Ruhr-Universität Bochum, 44780 Bochum,
    Germany
[18] Institute of Particle and Nuclear Physics, Charles University, V Holesovickach 2, 180 00 Prague 8, Czech Republic
[19] University of Namibia, Private Bag 13301, Windhoek, Namibia
[20] European Associated Laboratory for Gamma-Ray Astronomy, jointly supported by CNRS and MPG

* Université Libre de Bruxelles, Faculté des Sciences, Campus de la Plaine, CP 230, Boulevard du Triomphe, 1050 Bruxelles, Belgium.
** Now at Washington Univ., Department of Physics, 1 Brookings Dr., CB 1105, St. Louis, MO 63130, USA.
*** Now at Department of Physics and Astronomy, Univ. of Sheffield, The Hicks Building, Hounsfield Road, Sheffield S3 7RH, UK.

Abstract. The region around PSR B1706–44 has been observed with the HESS imaging atmospheric Cherenkov telescopes in 2003. No evidence for γ-ray emission in the TeV range was found at the pulsar position or at the radio arc which corresponds to the supernova remnant G 343.1–2.3. The 99% confidence level flux upper limit at the pulsar position is $F_{ul}(E > 350 \text{ GeV}) = 1.4 \times 10^{-12} \text{ s}^{-1} \text{ cm}^{-2}$ assuming a power law ($\mathrm{d}N/\mathrm{d}E \propto E^{-\Gamma}$) with photon index of $\Gamma = 2.5$ and $F_{ul}(E > 500 \text{ GeV}) = 1.3 \times 10^{-12} \text{ s}^{-1} \text{ cm}^{-2}$ without an assumption on the spectral shape. The reported upper limits correspond to 8% of the flux from an earlier detection by the CANGAROO experiment.

Key words. gamma rays: observations – ISM: individual objects: PSR B1706–44 – ISM: supernova remnants – ISM: individual objects: G 343.1–2.3

1. Introduction

PSR B1706–44 is a young pulsar (spin-down age of ~17 kyr) with distance estimates ranging from 1.8 to 3.2 kpc with a period of 102 ms and a spin-down luminosity of about 1% of the Crab pulsar ($3.4 \times 10^{36} \text{ erg s}^{-1}$). Pulsed emission has been observed at radio and X-ray wavelengths, and in GeV γ-rays. An extended synchrotron nebula around this compact object has been found in radio observations (Giacani et al. 2002) with an extension of $1'$–$4'$ and with a flat spectrum (energy index of 0.3), and also in X-rays (Gotthelf et al. 2002) with an extension of ~20″ and with a photon index of 1.34. These characteristics suggest the existence of a pulsar wind nebula (PWN) powered by the pulsar. In the TeV range, the CANGAROO experiment detected a steady emission coincident with the PWN position at a level of roughly 50% of the Crab flux (Kifune et al. 1995; Kushida et al. 2003), suggesting that this PWN is the southern equivalent of the Crab nebula. The Durham Mark 6 collaboration (Chadwick et al. 1998) reported also a significant detection above 300 GeV. A flux upper limit above 500 GeV which is compatible with the CANGAROO flux has been derived using data from the BIGRAT telescope (Rowell et al. 1998).

PSR B1706–44 is coincident with an incomplete arc of radio emission (McAdam et al. 1993) which has been interpreted as a shell-type supernova remnant (SNR) named G 343.1–2.3. This SNR has been detected only at radio wavelengths (Duncan et al. 1995) and may be associated with the pulsar as discussed in Bock & Gvaramadze (2002).

We present here the results of the observation of the field of view around PSR B1706–44 with the HESS experiment. HESS is an atmospheric Cherenkov detector dedicated to the observation of TeV γ-rays (Hofmann 2003). Situated in Namibia, the full four-telescope array is operational since December 2003. Each telescope has a mirror area of 107 m^2 (Bernlöhr et al. 2003) and is equipped with a camera consisting of 960 photomultiplier tubes (PMT) (Vincent et al. 2003). The system has a field of view of 5°. In stereoscopic observation mode, it allows one to reconstruct the direction of individual showers with a precision better than 0.1°.

2. Observations and data analysis

PSR B1706–44 was observed with two HESS telescopes between April and July 2003. During this commissioning phase, GPS time stamps were used in the offline data analysis to identify showers observed in coincidence by the two telescopes. This coincidence requirement allows for a higher background rejection and thus for a better sensitivity than single telescope

observations. In this configuration, a source with a flux of 5% of Crab nebula can be detected with more than 5σ in 4.5 hours at 20° zenith angle. The pulsar was observed with 28-min runs in wobble mode, whereby runs are taken pointing ±0.5° away from the pulsar position in declination. Data affected by hardware problems or bad weather conditions were excluded from analysis. The proper functioning of the detector system was verified by numerous checks. The telescope pointing has been confirmed by correlating high PMT currents with bright stars in the field of view. The trigger rate of the system is well reproduced by simulations for cosmic rays, and the shape of simulated γ-ray images is consistent with the result of Crab observations. Data analysis is performed with two completely independent chains with different calibrations, with independent Monte Carlo simulations and with different analysis techniques.

The selected data have a total live time of 14.3 h. The energy threshold estimated from Monte Carlo simulations at the average observation zenith angle (~26°) is about 350 GeV. This threshold is higher than for the four-telescope system since the telescopes were operated with higher trigger thresholds in the commissioning phase. Data were analysed using standard shower reconstruction and standard background rejection methods (Aharonian et al. 2005). Standard cuts, optimised on Monte Carlo simulations, have been applied on mean scaled Hillas parameters in order to increase the signal-to-background ratio. Showers were classified using the angular distance θ between their reconstructed direction and the direction of possible source. For this standard analysis, showers were accepted as coming from the source (the ON region) when their θ^2 was smaller than 0.02 degree^2 (i.e. angular distance smaller than 8.5′). The background was determined by counting events in a ring (the OFF region) centered at the investigated direction whose inner radius is larger (>0.4°) than the θ^2 cut and whose area is 7 times larger than the ON region. A normalization factor α is applied to these estimated background counts to correct for the different size of ON and OFF regions and the different radial acceptance in the field of view.

3. Results

A plot of θ^2 relative to the PWN position is shown in Fig. 1. The significance, calculated according to Li & Ma (1983), is 0.1 σ. Table 1 provides an overview of the event statistics in the column labelled *Standard*. The analysis described above was repeated with the same cuts for every point in the field of view. The resulting significance map is presented in Fig. 2. It exhibits no significant point source excess in the vicinity of the pulsar or on the radio emission arc.
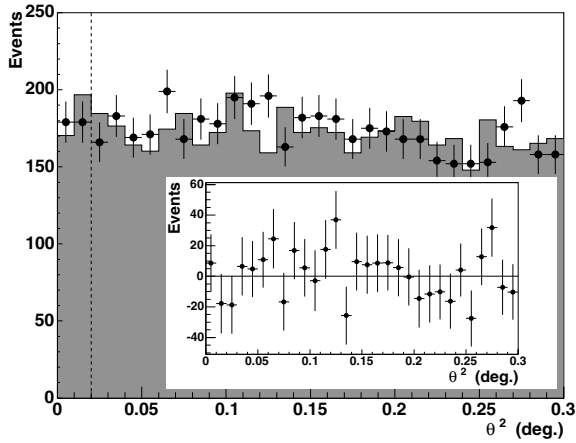
Fig. 1. θ^2 distribution calculated with respect to the PWN position. The dots denote events from the ON region, the histogram are the events from the OFF region scaled by the normalization factor α. The dashed vertical line indicates the applied angular cut. The inset shows the difference between the ON and the scaled OFF regions.

Table 1. Analysis results: $N_{\rm on}$ and $N_{\rm off}$ are the event numbers in the ON and OFF regions, α is the normalisation factor. The results are reported for the standard θ^2 cut (column labelled *Standard*), for the cuts reproducing the conditions of the CANGAROO detection (column *CANGAROO*) and for the analysis of the radio arc (column *Radio arc*).

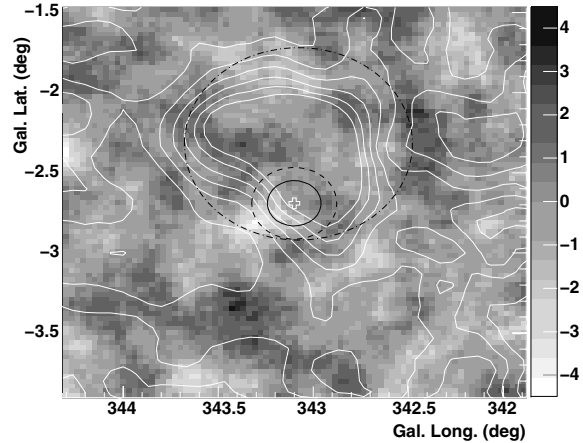|	*Standard*	*CANGAROO*	*Radio arc*
$N_{\rm on}$	352	112	4746
$N_{\rm off}$	2243	512	13 688
α	0.15620	0.19258	0.34592
Excess	1.6 ± 20.2	13.4 ± 11.1	11.0 ± 79.9
Significance	0.1σ	1.2σ	0.1σ

Fig. 2. Significance map centered on PSR B1706–44. The cross marks the pulsar position. The contour lines correspond to the 2.2 GHz image of G 343–2.3 (Duncan et al. 1995). The solid circle indicates the integration region of the *Standard* cuts, the dashed circle the *CANGAROO* cuts and the dot-dashed circle the *Radio arc* cuts. The significance distribution for the entire HESS field of view is compatible with a Gaussian of mean −0.06 and of sigma 1.09.

Table 2. Flux upper limits at 99% confidence level for the pulsar position in s^{-1} cm^{-2}. The upper limits from Method A were calculated assuming a photon index of $\Gamma = 2.5$. The numbers in parentheses are the energy thresholds (in TeV) for which the upper limits were determined.

	Method A		Method B	
Standard	1.4×10^{-12}	(0.35)	1.3×10^{-12}	(0.50)
CANGAROO	6.4×10^{-13}	(1.00)	7.7×10^{-13}	(1.00)
Radio arc	5.8×10^{-12}	(0.35)	3.5×10^{-12}	(0.50)

In order to roughly reproduce the conditions of the PSR B1706–44 detection by CANGAROO, the analysis at the pulsar position was repeated using a looser θ^2 cut of 0.05 degree^2 and selecting events above an energy of 1 TeV. The results are shown in the column labelled *CANGAROO* of Table 1 and give no indication for a significant excess. For the analysis of the radio arc, a θ^2 cut of 0.36 degree^2 has been applied around the position (17h08m, $-44°17'$) and no significant excess is measured (column labelled *Radio arc* of Table 1).

Limits on the integral flux above certain energies E_T were obtained using two different methods. The first method (Method A) tests the hypothesis that the number of excess events with energies above E_T result from a source with a power law spectrum with a (positive) photon index Γ. The photon index was varied between 2 and 3. This range includes the value of $\Gamma = 2.5$ from the earlier CANGAROO detection. The second method (Method B) makes no assumption about the source spectrum and calculates the integrated flux F directly as the difference of the measured flux from the ON region and the flux of cosmic-rays from the OFF region:

$$F(>E_T) = \frac{1}{T}\left(\sum_{i=1}^{N_{\rm on}} \frac{1}{A_i} - \alpha \sum_{i=1}^{N_{\rm off}} \frac{1}{A_i}\right).$$

Here, T is the live time, and both sums on the ON and OFF regions run over all showers with reconstructed energies greater than E_T. The effective areas (A_i) depend on the zenith angle and energy of each event, and α is the normalization factor. As A_i is determined using the reconstructed energy, the energy threshold should be increased such that the bias of the reconstructed energy is less than 10%. The upper limits derived with both methods were calculated using the unified approach of Feldman & Cousins (1998) and a confidence level of 99%. To compare the upper limits from Method B with a prediction, the investigated model spectrum must be integrated over all energies starting at E_T.

Table 2 gives the values of flux upper limits at 99% confidence level for various cuts and methods; both methods give similar results. With method A, the upper limit at the PWN position corresponds to ~1% of the flux from the Crab Nebula (at the same energy threshold) and the upper limit for the radio arc corresponds to ~5% of the flux from the Crab Nebula. The upper limit which reproduces the experimental conditions of the CANGAROO experiment corresponds to ~8% of the flux reported by that collaboration.
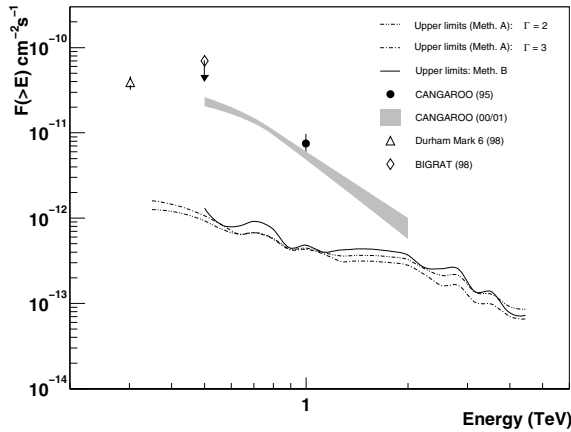
Letter to the Editor

Fig. 3. Integral upper limits at 99% CL for the flux from the PWN position (solid, dotted and dot-dashed line). The filled circle corresponds to the CANGAROO detection of Kifune et al. (1995) and the CANGAROO integrated flux (grey area) is calculated from the result of a broken power law fit to the 2000 and 2001 differential spectrum (Kushida et al. 2003). The open diamond and the triangle are from Rowell et al. (1998) and Chadwick et al. (1998), respectively.

4. Discussion and conclusions

The reported upper limits on the flux of TeV γ-rays are roughly one order of magnitude lower than the reported CANGAROO flux and a factor of 55 lower than earlier limits (Rowell et al. 1998). The CANGAROO observations were not contemporaneous with the HESS observations, which raises the question of whether the TeV emission could be variable on a time scale of years. Such a variability seems unlikely given our current understanding of PWN (Blondin et al. 2001). Another potential reason for the discrepancy could be an object confusion along the line of sight. There are, however, no BL Lac objects or variable galactic TeV γ-ray emitters known around the pulsar. It has been pointed out (Aharonian et al. 1997; Kushida et al. 2003) that the high flux level reported by CANGAROO is surprising. Since the X-ray luminosity is about 0.01% of that of the Crab PWN, the TeV γ-rays should be emitted from a much larger volume than the X-rays, according to the inverse Compton (IC) scenario.

Using the HESS flux upper limit above 1 TeV, a lower limit on the magnetic field can be derived from Eq. (6) of Aharonian et al. (1997). This requires a measurement of the flux in the X-ray band from the same electron population that emits the hypothetical TeV radiation. Measurements by Chandra (Gotthelf et al. 2002) provide a flux from the PWN, excluding the point-like emission of the central source; however, their chosen analysis region (radius less than 10″) is smaller than the full extent of the PWN, for which Finley et al. (1998) found a best-fit exponential scale length of 27″. The flux measured by ASCA (Finley et al. 1998) encompasses the entire PWN, but also includes the pulsar emission. To estimate the PWN flux, we used the ASCA spectrum but subtracted a point source contribution estimated from ROSAT HRI to be (43 ± 12)% (Finley et al. 1998), yielding an unabsorbed flux of 5.5×10^{-13} erg s^{-1} cm^{-2} in the 2–10 keV band for the PWN. The lack of observable X-ray emission below about 0.5 keV

due to interstellar absorption means that the electrons producing the observed X-rays have somewhat higher energy than those producing TeV γ-rays, and an extrapolation of the X-ray spectrum to lower energies is necessary. The spectral index measured with ASCA, $\Gamma = 1.7^{+0.5}_{-0.4}$, is fully compatible with the more precise determination from BeppoSAX, $\Gamma = 1.69 \pm 0.29$ (Mineo et al. 2002). The derived lower limit on the magnetic field strength is then about $1\,\mu$G when one assumes that the inverse Compton scattering involves only the photons of the microwave background radiation and assuming the same photon index in the X-ray and TeV band. This value is however not very constraining given that the mean Galactic magnetic field is of the same order of magnitude.

References

Aharonian, F., Atoyan, A. M., & Kifune, T. 1997, MNRAS, 291, 162
Aharonian, F., Akhperjanian, A. G., Aye, K.-M., et al. 2005, A&A, 430, 865
Becker, W., Brazier, K. T. S., & Trümper, J. 1995, A&A, 298, 528
Bernlöhr, K., Carrol, O., Cornils, R., et al. 2003, APh., 20, 111
Blondin, J. M., Chevalier, R. A., & Frierson, D. M. 2001, ApJ, 563, 80
Bock, D. C.-J., & Gvaramadze, V. V. 2002, A&A, 394, 533
Chadwick, P. M., Dickinson, M. R., Dipper, N. A., et al. 1998, APh, 9, 131
Duncan, A. R., Steward, R. T., Haynes, R. F., & Jones, K. L. 1995, MNRAS, 277, 36
Feldman, G. J., & Cousins, R. D. 1998, Phys. Rev. D, 57, 7
Finley, J. P., Srinivasan, R., Saito, Y., et al. 1998, ApJ, 493, 884
Giacani, E. B., Frail, D. A., Goss, W. M., & Vieytes, M. 2001, AJ, 121, 313
Gotthelf, E. V., Halpern, J. P., & Dodson, R. 2002, ApJ, 567, L125
Hofmann, W. 2003, Proc. 28th ICRC, Tsukuba (Tokyo: Univ. Academy Press), 2811
Kifune, T., Tanimori, T., Ogio, S., et al. 1995, ApJ, 438, L91
Kushida, J., Tanimori, T., Kubo, H., et al. 2003, Proc. 28th Int. Cosmic Ray Conf., Tsukuba (Tokyo: Univ. Academy Press), 2493
Li, T.-P., & Ma, Y.-Q. 1983, ApJ, 272, 317
McAdam, W. B., Osborne, J. L., & Parkinson, M. L. 1993, Nature, 361, L516
Mineo, T., Massaro, E., Cusumano, G., & Becker, W. 2002, A&A, 392, 181
Rowell, G. P., Dazeley, S. A., Edwards, P. G., Patterson, J. R., & Thornton, G. J. 1998, APh, 194, 332
Vincent, P., Denance, J.-P., Huppert, J.-F., et al. 2003, Proc. 28th ICRC, Tsukuba (Tokyo: Univ. Academy Press), 2887